Spatially resolved microdiffraction in hydrodynamic focusing microdevices[1, 2, 3, 4] provide new opportunities to study time-resolved reaction dynamics of complex fluids under controllable conditions. Aside from having advantages such as reduction of sample volumes and shorter reaction and analysis times, microfluidics is a powerful tool for investigations of soft condensed matter and biological systems. The characterization of these materials, which are typically liquid-crystalline at ambient conditions, is significantly improved owing to a concurrent orientation during self assembly processes.[1, 2] However, a major obstacle for performing X-ray diffraction measurements directly on a microfluidic chip is the lack of cheap and robust devices with thin low-absorbing and low-scattering windows suitable for X-ray measurements, which provide the ability of adapting the microchannel design according to the needs of each analyzed system. Therefore, we developed a straightforward and scalable method of fabricating long lifetime X-ray microdiffraction compatible microfluidic devices with thin polyimide (Kapton) windows (53µm).[5] The diversity of accessible channel geometries using microflow foils is demonstrated in figure 1a. The channel structure consists of a crossing area where three incoming channels meet followed by a meandering channel section consisting of successive U-shaped turns. Four hyperbolically shaped channel contractions down to 50µm in width are positioned horizontally along the channels. Due to the winding channel course, it is possible to extend the length of the channel significantly without increasing the total lateral dimensions of the flow cell. Thus, it is possible to adjust the residence time of the analyzed molecules in the channel individually to their reaction times. Furthermore, the microflow foils provide the possibility to integrate an unlimited number of inlets on one microfluidic device enabling the investigation of hierarchical self-organization of biomaterials in which normally a multitude of components is involved. To test and to demonstrate the analytic power and the possibilities offered by these microflow foils, we performed X-ray microdiffraction measurements in order to study shear-induced alignment effects in the well characterized smectic liquid crystal *n*-octyl-4-cyanobiphenyl (8CB) system.

8CB is injected in all three inlet channels. Using the synchrotron microdiffraction setup with a beam size of 20µm, two dimensional diffraction patterns of the 8CB smectic A layers at different positions within the microfluidic device can be obtained with a high spatial resolution corresponding to the beam size. Applying a flow velocity of $500\mu ms^{-1}$ (mean shear rate $0.5s^{-1}$), a width $w = (15.6 \pm 0.6)°$ is observed in regions with parallel channel geometry. Figure 1b shows measurements perpendicular to the channel at a position close to the end of a hyperbolic section., a decrease in width of the azimuthal intensity distribution down to $w = (5.9 \pm 0.6)°$ is observed when approaching maximum flow velocity in the middle of the channel. This demonstrates the strong shear-induced ordering of 8CB. Furthermore, the orientational distribution as a function of the *y*-position shows experimentally the orientation of the complex material along the stream lines.

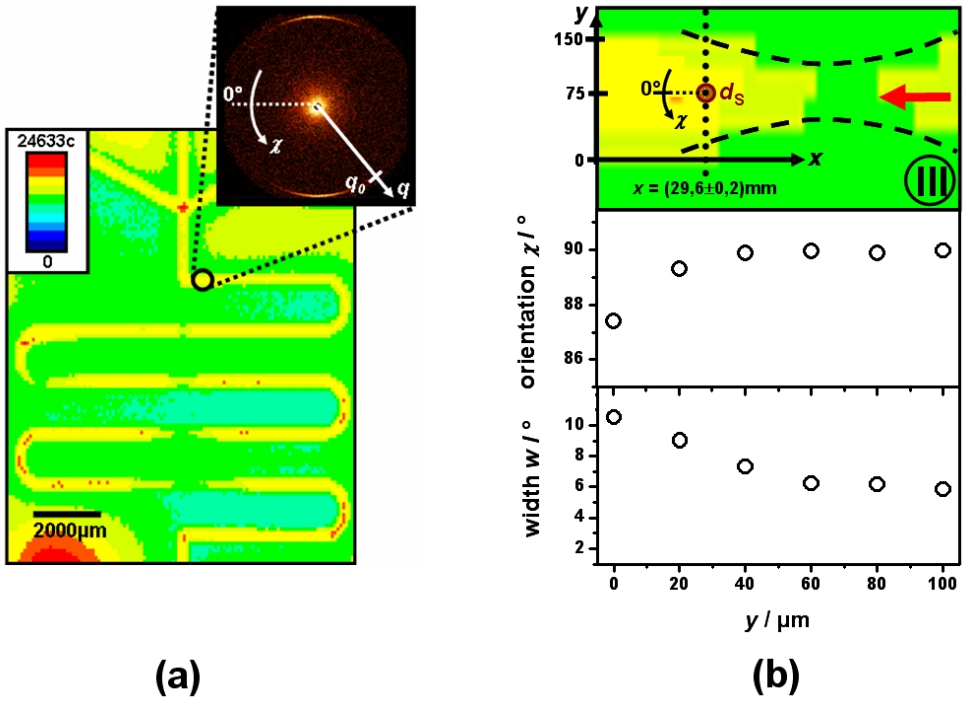

Figure 1: a) X-ray absorption scanning image (step size 0.1µm, exposure time 0.5s) of the microfluidic channel system using an in-house setup with a beam size of 200µm. The channel structure is observable due to the lower absorption of 8CB compared to PDMS. The inset picture shows the 2D liquid crystalline diffraction pattern of 8CB with a smectic A layer spacing of $q_0 = 0.198Å^{-1}$. b) Orientation χ and width w of the azimuthal intensity distribution along the y axis perpendicular to the channel, measured using a flow velocity of $500µms^{-1}$ and a microfocused X-ray beam with a diameter $d_s \approx 20µm$. The top section shows the corresponding channel domain, the red arrow indicates the flow direction.

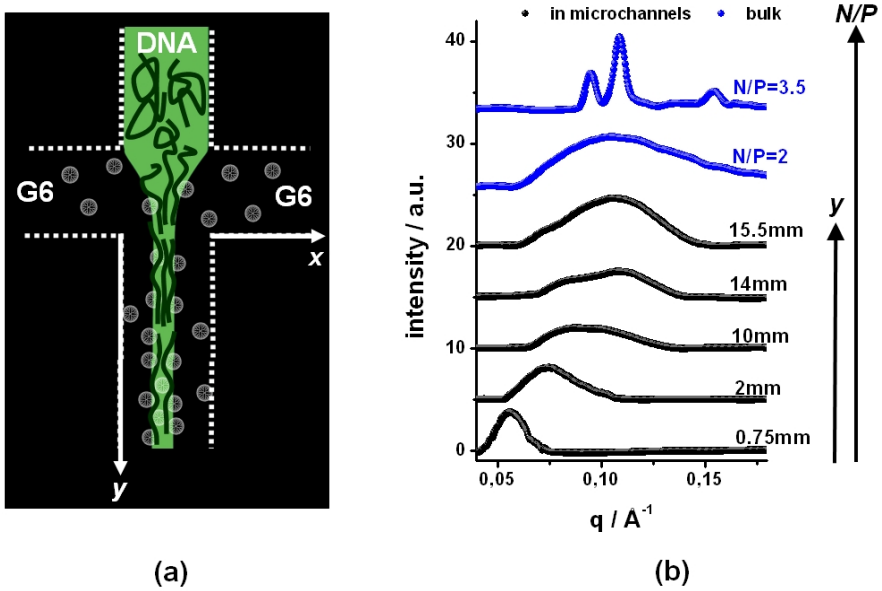

Figure 2: a) Schematic representation of the experiment. b) Series of small angle X-ray microdiffraction measurement of the DNA compaction by PAMAM dendrimers generation 6. Data represented black is obtained from measurements in the microchannel device, data shown in blue originates from bulk measurements.

In previous experiments we investigated the compaction of DNA by dendrimers generation 4 (3.12nm in diameter). As a next step towards understanding the hierarchical organization of chromatin, we use the microflow foils for analyzing DNA compaction by PAMAM dendrimers generation 6 (P6, 4.7nm in diameter). A semi-diluted aqueous solution of DNA is injected in the centre channel and hydrodynamically focused by two side streams containing aqueous solutions of P6 dendrimers (figure 2). Owing to the diffusive mixing behaviour, different local concentrations exist along and perpendicular to the hydrodynamically focused DNA stream. Changes in the relative charge ratio N/P which is known to influence the structure of formed aggregates are correlated with these concentration variations. Here, N denominates the number of positive amine charges of the dendrimers (assuming full protonation) whereas P is the number of the negative phosphate charges of the DNA backbone. Different N/P ratios and therefore different aggregation states are observable along the outlet channel. Therefore, different time frames of the mixing reaction are accessible by varying the observation position along the outlet channel.

At a position $y = 0.75$mm after the intersection, the DNA-DNA correlation peak corresponding to an interhelical distance of 113Å is visible. The position of this peak is shifted towards higher q values and the peak broadens when moving along the outlet channel. At $y = 10$mm a second broad peak arises at $q = 0.1028$Å^{-1} which is successively moving towards higher q values ($q = 0.1061$ Å^{-1} at $y = 15.5$mm) with increasing N/P ratio. The packing of the DNA chains lacks long-range positional order as the corresponding DNA-DNA correlation peak is broad. We hence designated the mesomorphic structure as a nematic phase. To rule out the N/P ratio at the final channel position y =15.5mm, the scattering data is compared with results from bulk measurements, revealing an N/P ratio of 2. Increasing the N/P ratio further, the P6/DNA complex is found to undergo a structural transition from a condensed nematic phase ($N/P = 2$) to a long range ordered columnar phase ($N/P = 3.5$). Here, the SAXS profile shows three distinct peaks located at $q_1 = 0.094$Å^{-1}, $q_2 = 0.1093$Å^{-1} and $q_3 = 0.1543$Å^{-1}, respectively. The ratio of the positions $q_3/q_2 = 1.412$ corresponds closely to the lattice scattering from a 2D square columnar phase with the lattice constant of 57.5Å. This 2D square columnar phase coexists with a hexagonal phase with a lattice constant of 66.8Å indicated by the corresponding primary peak at q_1. To rule out the nature of this coexistence in more detail, further experiments are on the way.

In a third set of experiments, a 3D network of fibrin is formed in a microchannel device and monitored in real time using X-ray microdiffraction. The network is formed due to the activation of monomers of fibrinogen by the enzyme thrombin (figure 3a). The formation of fibrin fibrils results in a scattering peak at $q = 0.295$nm^{-1}, which originates from the repeat unit $d \approx 22$nm of the symmetric monomers within fibrils (figure 3a). The development of this feature is tracked as a function of position y along the channel, and two regimes are noted: First, the increasing intensity of the fibrils until a distance of 1mm and second, constant peak intensity at further distances. The transition point between these regimes occurs at a distance (1mm) where the concentration of thrombin is constant. Given these promising results, this technique should also be able to access dynamic formation of fibrils with the use of more dilute enzyme concentrations.

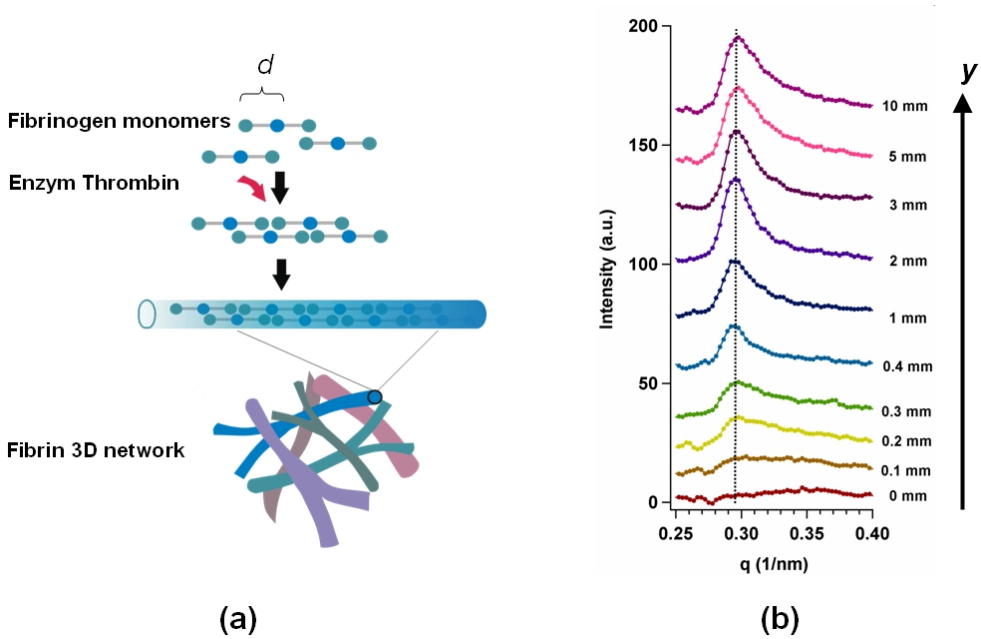

Figure 3: a) Schematic representation of the 3D fibrin network formation. b) Series of small angle X-ray microdiffraction measurement of the self-assembly of the fibrin network at different positions along the outlet channel.

---

[1] R. Dootz, A. Otten, S. Köster, B. Struth, T. Pfohl, *J. Phys. Cond. Matter* **2006**, *18*, S639
[2] S. Köster, J. B. Leach, B. Struth, T. Pfohl, J. Y. Wong, *Langmuir* **2007**, *23*, 357.
[3] B. Struth, A. Snigirev, O. Konovalov, A. Otten, R. Gauggel, T. Pfohl, *‚AIP Conf. Proc. SRI* **2003**, *705*, 804.
[4] A. Otten, S. Köster, B. Struth, A. Snigirev, T. Pfohl, *J. Synchrotron Rad.* **2005**, 12, 745.
[5] R. Dootz, H. Evans, S. Köster, T. Pfohl, *Small* **2007**, *3*, 96.